Synthesis of nickel–rubber nanocomposites and evaluation of their dielectric properties

E. Muhammad Abdul Jamal[a], P.A. Joy[b], Philip Kurian[c], M.R. Anantharaman[a],*

[a] Department of Physics, Cochin University of Science and Technology, Cochin 682022, India
[b] National Chemical Laboratory, Pune, India
[c] Department of Polymer Science and Rubber Technology, Cochin University of Science and Technology, Cochin 22, India

ARTICLE INFO

ABSTRACT

Nanocomposites based on natural rubber and nano-sized nickel were synthesized by incorporating nickel nanoparticles in a natural rubber matrix for various loadings of the filler. Structural, morphological, magnetic and mechanical properties of the composites were evaluated along with a detailed study of dielectric properties. It was found that nickel particles were uniformly distributed in the matrix without agglomeration resulting in a magnetic nanocomposite. The elastic properties showed an improvement with increase in filler content but breaking stress and breaking strain were found to decrease. Dielectric permittivity was found to decrease with increase in frequency, and found to increase with increase in nickel loading. The decrease in permittivity with temperature is attributed to the high volume expansivity of rubber at elevated temperatures. Dielectric loss of blank rubber as well as the composites was found to increase with temperature.

1. Introduction

It is well known that the dielectric properties of an insulating medium can be modified by dispersing electrically conducting particles in the medium [1–4]. The insulating host material can in turn be made conducting or semi-conducting, depending on the amount of filler particles dispersed in the medium [5]. Magnetic fillers are incorporated in rubber matrices to impart magnetic property to the host and such fillers can be metal particles or magnetic oxides like ferrites [6–8]. When magnetic oxides are used, very high volume fraction of the filler is necessary to get the required magnetization because of the low density of oxides in comparison to metals. High volume fraction of the filler can deteriorate the physical properties of the polymer material. One way to overcome this difficulty is to use metal particles as filler. Ferromagnetic iron, nickel or cobalt particles are the choices as metallic magnetic filler materials. Nickel particles are chemically more stable and therefore make a better choice.

Elastomers are flexible materials and composites of these materials can find many useful technological applications mainly due to their flexibility and mouldability [8]. Natural rubber is a commonly available elastomer and there exist reports on the studies on electrical properties of composites based on natural rubber with ferrite particles as fillers [7,8]. However reports on the synthesis of composites of natural rubber dispersed with metal particles are not very abundant in the literature.

In this article we describe the synthesis of nickel-filled rubber composites which have magnetic as well as dielectric properties. The volume ratio of filler is below the percolation threshold in order to make these composites purely dielectric materials. Nickel, being metallic can alter the dielectric properties of rubber and at the same time, being ferromagnetic can impart high magnetic permeability to the composites. These composites can be used as flexible magnets, and the mouldability of rubber gives a high degree of freedom in terms of shape and size. Being magnetic and dielectric at the same time, they have the potential to be used in applications like electromagnetic interference shielding and electrostatic charge dissipaters [1]. Rubber is inexpensive, and the possibility of synthesizing materials capable of absorbing electromagnetic radiation from rubber assumes importance because of its cost effectiveness. Evaluation of the magnetic and dielectric properties of the material is equally important to assess the usability of the material in applications. In addition to the structural, magnetic, morphological and mechanical properties, we attempt to make a detailed evaluation of the dielectric properties of the composites in the frequency range of 100 kHz to 8 MHz. The evaluation of the dielectric behaviour at radio frequency range assumes importance from the point of view of using these materials in low frequency electronic components. These studies can also reveal the influence of interfacial polarization in determining the dielectric permittivity of compos-

* Corresponding author. Tel.: +91 484 2577404; fax: +91 484 2577595.
E-mail address: mraiyer@yahoo.com (M.R. Anantharaman).

ite materials, and the influence of metallic inclusions in altering the dielectric permittivity in natural elastomers like rubber.

There are many factors which influence the dielectric and conducting properties of insulator–metal composites [5,9]. The most important of these is the ratio of the filler particles to the host material. At lower volume ratios, the composites are good dielectric materials, but the conductivity of the material can increase sharply at some critical value of the volume ratio. This is due to the formation of conductive paths at the percolation threshold of the filler particles [10]. But within the percolation threshold, these materials are good insulators, and their dielectric properties can be tuned by the volume ratios of the filler material. The investigations of dielectric properties of metal elastomer composites thus assume importance under these circumstances.

2. Experimental details

2.1. Materials

Natural rubber gum was used as the matrix. Compounding ingredients like sulphur, stearic acid, and zinc oxide were utilized according to a specific recipe evolved by trial and error. For the synthesis of nickel nanoparticles, nickel nitrate hexahydrate and ethylene glycol were purchased from Merck, India and used without any further purification.

2.2. Synthesis of nickel particles

Nickel particles were synthesized by the authors using a modified sol–gel combustion process (patent pending–patent No. 1927/07/Indian patent) similar to a process reported earlier [11]. Smaller particle size can be obtained by employing this modified process. The synthesized powder was subjected to high-energy ball-milling using a Fritsch planetary ball mill model P-7 for around 2 h to further reduce the size of the particles well below 100 nm.

2.3. Preparation of composites

The curing of the rubber samples was carried out as per ASTM procedure reported elsewhere [12]. A series of five nickel–rubber composite samples were synthesized with varying concentrations of nickel ranging from 20 phr to 100 phr (per hundred weight ratio of rubber) along with a sample of blank rubber vulcanisate for comparative studies. Natural rubber along with the compounding ingredients and the nickel filler were mixed in a Brabender Plasticoder according to a specific recipe at 60 °C. The compound material was removed from the mixing chamber and further homogenization was carried out in a two-roll mill operated with a friction ratio of 1:1.25. The compound was endwise passed six times through the two-roll mill, with a tight nip and finally rolled into a sheet by keeping the nip at a separation of 3 mm. These sheets were kept for 24 h before evaluating the cure characteristics. The cure times were determined for each composite sample separately using a rubber process analyzer (RPA2000 of α-Technology). The samples were moulded in the form of sheets of thickness 2 mm at a temperature 150 °C.

2.4. Initial characterization of nickel nanoparticles and the composites

The evaluation of the structural properties of nickel particles was carried out by means of an X-ray diffractometer (XRD) (Rigaku Dmax C with Cu Kα X-ray source of wavelength of 1.54 Å). Superconducting quantum interference device magnetometry (SQUID)

was employed for evaluating the magnetic properties (MPMS-5S XL Quantum Design magnetomer) and transmission electron microscopy (TEM) (PHILIPS CM200 operating at 20–200 kV with a resolution of 2.4 Å) was utilized to study the particle size and shape. After the preparation of the composites, their structure was analyzed using XRD. Vibrating sample magnetometry (VSM) (EG&G PAR 2000 VSM) was employed to study the magnetic properties of the composites. Scanning electron microscopy (SEM) (JEOL model JSM–6390LV) was used to study the morphology of the composites. The mechanical properties of the composites as well as the blank rubber were carried out by a universal testing machine (UTM) (model Instron 4500) using dumb-bell-shaped sheets cut according to ASTM standards.

2.5. Dielectric studies

Circular discs were cut out from the cured sheets of composites with a diameter of 12 mm for dielectric studies. These studies were carried out using a HP impedance analyzer model 4285 A in the frequency range of 100 kHz to 8 MHz by varying the temperature from 30 °C to 120 °C. The samples were inserted between two copper plates of the same diameter to form a capacitor in a home-made dielectric cell whose fabrication details are reported elsewhere [13]. Using the impedance analyzer the capacitance and loss tangent were recorded at intervals of 100 kHz using an automated measurement set-up. The measurement was automated by interfacing the impedance analyzer with a personal computer through a GPIB cable IEE488. A commercial interfacing and automation software LabVIEW was used for the acquisition of data. The program for data acquisition was written in the language G which is a graphical language much suitable for data acquisition applications. With this 20,000 data points can be acquired in a matter of 5 min and transported to a file. The dielectric permittivity of the sample was calculated using the relation [7]:

$$\varepsilon' = \frac{Cd}{\varepsilon_o A} \tag{1}$$

and the dielectric loss by the relation:

$$\varepsilon'' = \varepsilon' \tan \delta \tag{2}$$

where ε' is the dielectric permittivity of the sample (the real part), C is the capacitance of the capacitor formed by inserting the sample between two metal plates, d is the thickness of the sample, ε_o is the permittivity of free space, A is the area of cross section of the sample and δ is the loss tangent.

3. Results and discussions

3.1. Nickel particles

The results of XRD studies were used for the analysis of structural properties of the nickel particles. The XRD pattern was compared with the published results available in JCPDS files and it was found that the obtained pattern exactly matches with the reported result (JCPDS file no 03-1051). The diffraction peaks were identified and indexed. Particle size D was determined using Debye–Scherrer formula given as:

$$D = \frac{0.9\lambda}{\beta \cos \theta} \tag{3}$$

where λ is the wavelength of the X-ray source, β is the full width at half maximum of the diffraction peaks in radians, and 2θ is the diffraction angle [14]. The average particle size was evaluated and found to be 26 nm. The X-ray diffraction pattern of nickel particles is shown in Fig. 1. The magnetic hysteresis of nickel particles is
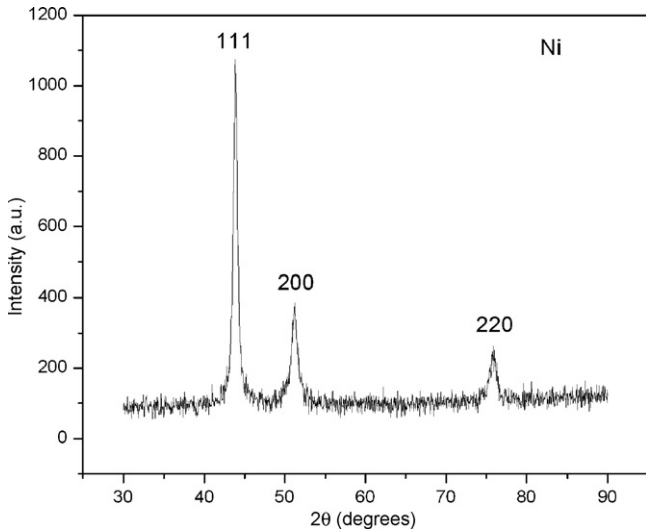
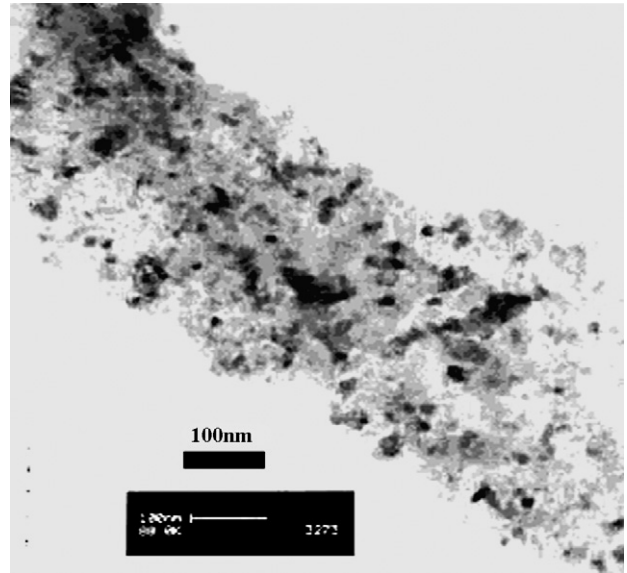**Fig. 1.** XRD pattern of nickel particles.

Fig. 3. TEM picture of nickel nanoparticles.

presented in Fig. 2. The result indicates that the particles are ferromagnetic with a coercivity of 68 Oe and a remnant magnetization of 8.5 emu/g. The saturation magnetization is found to be 47.5 emu/g and this also is about 87% of the magnetization of bulk nickel sample which was reported elsewhere [15]. The TEM micrograph shown in Fig. 3 establishes the formation of nickel particles in the range of 25–40 nm.

3.2. Nickel–rubber composites

The rubber composite samples were subjected to structural characterization immediately after they were moulded into sheets using X-ray diffractometry and the resulting XRD patterns are shown in Fig. 4. The characteristic peaks of nickel are clearly visible in all the samples. In the sample of 0 phr (blank rubber) a broad peak centered at 22° of 2θ is observed and this is due to the short-range orientation of polymer molecules of cured rubber [16]. Diffraction peaks marked 1–5 are due to various curing agents remaining unreacted in the blank rubber. The broad peak at 22° vanishes as we

increase the content of nickel since the large diffraction peaks of crystalline nickel with fcc structure become predominant. There are no shifts in the positions of the diffraction peaks of the nickel and this indicates that no structural change has occurred to the nickel particles due to the heat treatment. Peaks corresponding to NiO are present in the pattern and this indicates the presence of trace amounts of NiO which had arisen due to the heat treatment at 150 °C or due to heat generated while mixing. But this presence of NiO did not affect the magnetic properties of the composites in any significant manner. This was evident from the result of magnetic hysteresis studies on the composites at room temperature which is shown in Fig. 5. All samples were found to be ferromagnetic in nature. The as-prepared nickel nanoparticles have a magnetization of 47.5 emu/g and the magnetization of the composites was calculated taking the amount of nickel in the composites into account and by assuming that all other components in the composites are non-magnetic. The saturation magnetization of the composite can
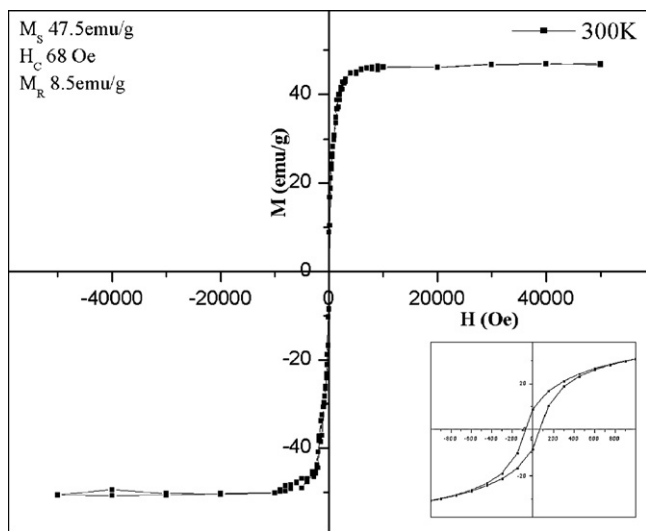

Fig. 2. Magnetic hysteresis of nickel particles. Figure in inset shows the central portion of the hysteresis loop enlarged to indicate the coercivity and remnant magnetization of the nickel particles.
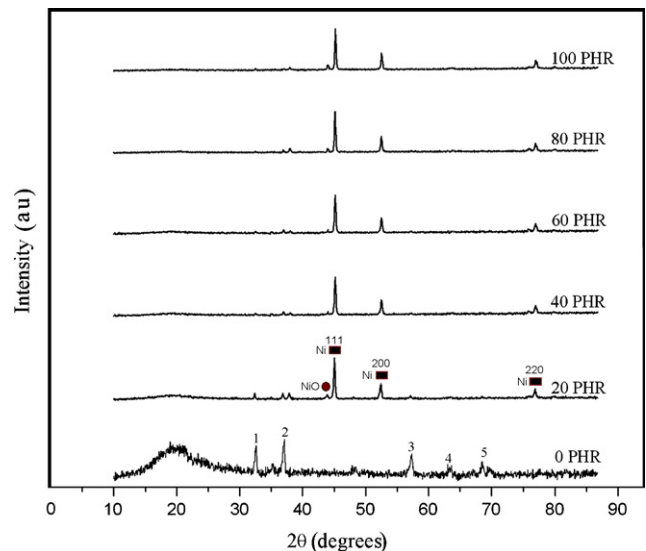

Fig. 4. XRD of nickel–rubber composites from 0 phr to 100 phr. Diffraction peaks marked with circles are that of NiO and rectangles are that of metallic nickel with fcc structure.
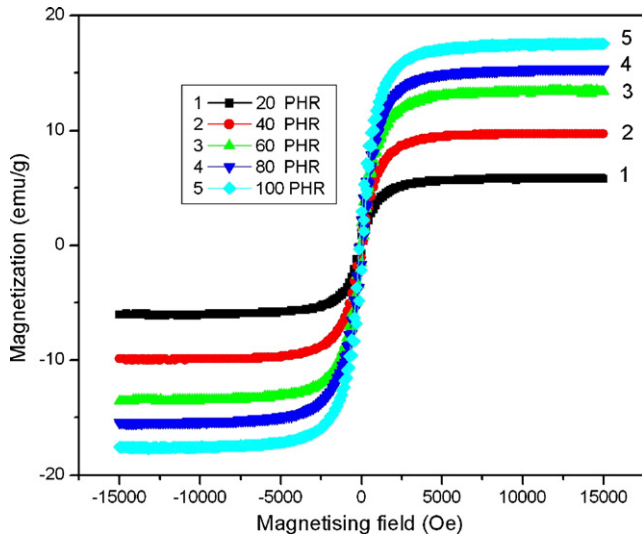
Fig. 5. Magnetic hysteresis of composites measured on VSM. The composites show a ferromagnetic behaviour and the saturation magnetization is found to increase with the nickel content.

be represented by the relation:

$$M_s(\text{composite}) = \frac{M_s(\text{nickel}) \times M_2}{M_1} \tag{4}$$

where, $M_s(\text{composite})$ is the saturation magnetization of the composite, $M_s(\text{nickel})$ is that of nickel particles, M_1 is the mass of a given sample of composite and M_2 is the mass of nickel particles in this sample. Calculated magnetization and the observed magnetization in each composite sample are tabulated and presented in Table 1. The observed magnetization values are in agreement with the calculated ones. Slight decrease in magnetization can be attributed to the loss of nickel particle while mixing, and the formation of traces of NiO at the time of curing. Scanning electron microscopy was carried out to study the morphology of the composite samples. A typical micrograph (of 100 phr sample) is presented as Fig. 6. This micrograph was taken on a fractured surface of rubber composite sample. Dispersion of the nickel particles can be observed in the picture. Two representative grains of nickel are indicated using arrows in Fig. 6.

3.3. Mechanical properties of nickel–rubber composites

Evaluation of the mechanical properties of the nickel rubber composites was carried out using a UTM (universal testing machine), model Instron 4500. Dumb-bell-shaped samples were cut using a sharp die with a cross section of 2 mm × 2 mm. Parameters namely tensile strength, modulus at different strains and elongation at the breaking point, which are some of the most important indications of the mechanical strength of the material were measured and the variations in these properties with loading were determined.
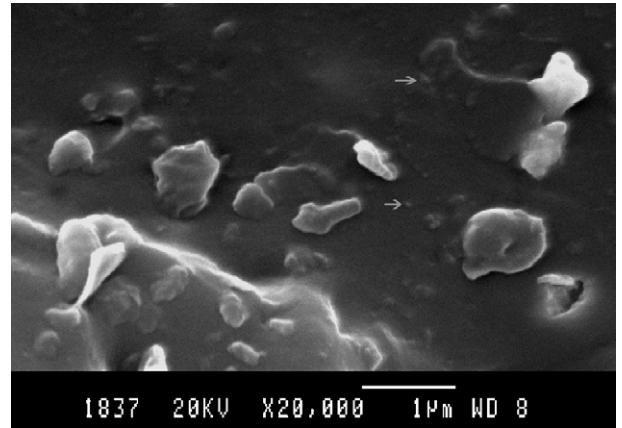

Fig. 6. SEM image of the composite of 100 phr sample.

The restoring stress developed inside the material for a particular strain is a good indicator of its mechanical strength. In Fig. 7 the stress of the composites for different strains is shown for various filler loadings. It was observed that the stress increased with the filler loading for all strains starting from 0.5 (50% elongation of the original length) to 3 (300% elongation). So it is clear that the incorporation of nickel nanoparticles in natural rubber matrix enhanced its elasticity. But there was a steady drop in stress at the breaking point (breaking stress) with increasing filler percentage as indicated in Fig. 8. The reason for this may be the microscopic discontinuities introduced in the matrix material due to the presence of the metal particles or the agglomerates of the particles. But the materials are not strained to the breaking point in its normal applications, and the lowering of breaking stress is not a demerit for the material in comparison to the enhancement in elastic properties.
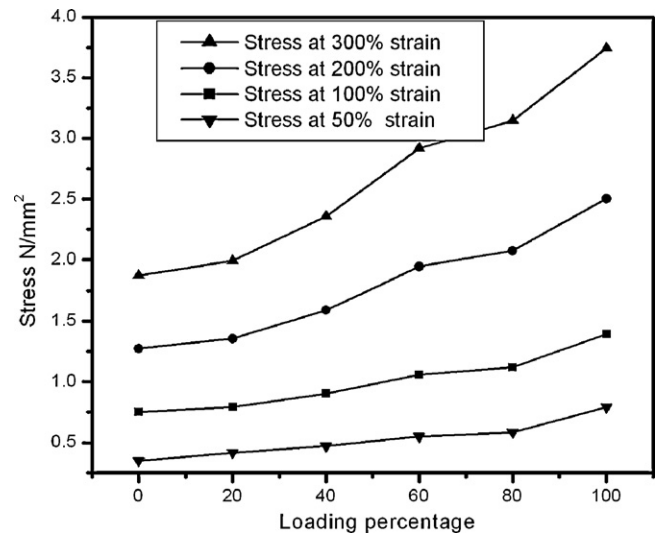

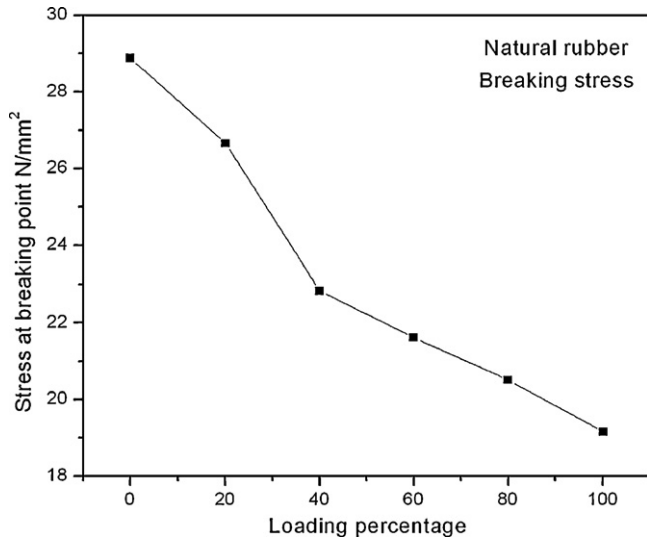**Fig. 7.** Variation of stress for different strains with filler loading.

Table 1
The observed and calculated magnetizations of the composites.

Sample (phr) (mass of nickel in 100 g rubber)	Total mass (nickel + rubber + curing agents)	Calculated magnetization (emu/g)	Observed magnetization (emu/g)
20	129.5	7.3	7
40	149.5	12.7	11
60	169.5	16.8	14
80	189.5	20	17.5
100	209.5	22.7	20

Fig. 8. Variation of breaking stress with filler loading.

Fig. 10. Variation of dielectric permittivity with frequency.

Again, from Fig. 9 it is clear that the strain at breaking point also drops off with the filler loading. But even at the minimum strain (for the 100 phr sample) the sample can be stretched to a length of 7.5 times of the original length. The composite breaks at lower elongations as the loading increases and this is one of the reasons for the drop in breaking stress.

3.4. Dielectric properties

Fig. 10 shows typical variation of dielectric permittivity of the samples within a frequency range of 100 kHz to 8 MHz at temperatures starting from 40 °C to 120 °C. The dielectric permittivity decreases almost linearly with frequency. At the lower side of the frequency the variation is slow and after about 2 MHz there is comparatively sharper variation and these variations are of the same nature at all temperatures. The graph shown as Fig. 10 is of 60 phr sample and the entire range of samples exhibit a similar behaviour. The drop in dielectric permittivity with increasing applied frequency is understood on the basis of Debye model of dielectric relaxation [17]. The behaviour of the dielectric constant of materials with a single relaxation mechanism can be represented by the
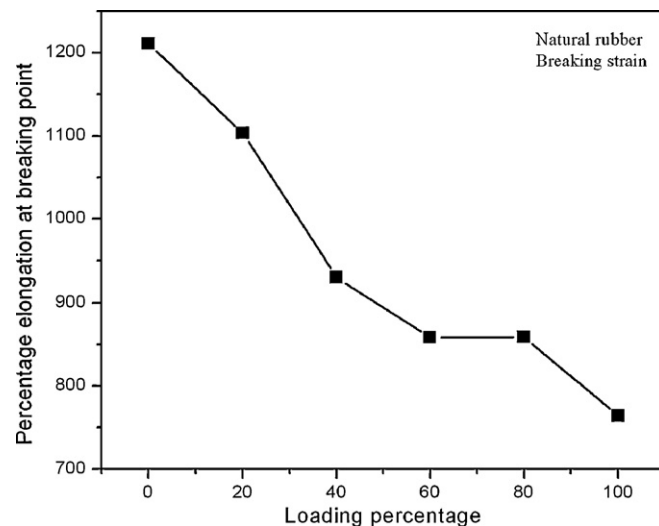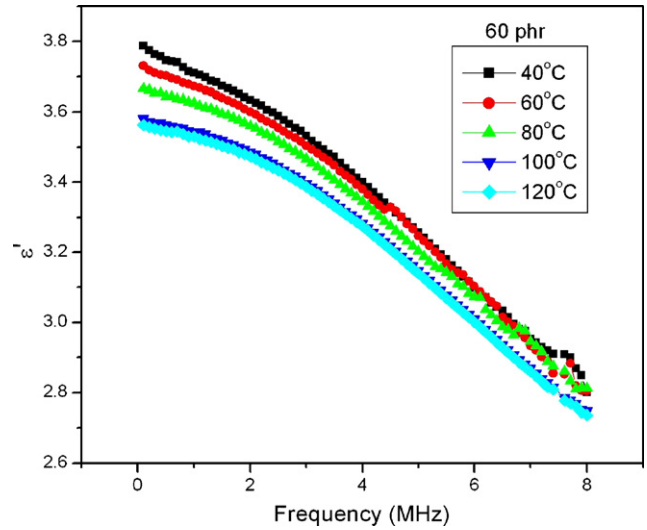
relation given in the form:

$$\varepsilon^*(\omega) - \varepsilon_\alpha = \frac{\varepsilon_s - \varepsilon_\alpha}{1 + i\omega\tau} \tag{5}$$

where $\varepsilon^*(\omega)$ is the complex permittivity at the frequency ω, ε_s is the static permittivity, ε_α is the permittivity at infinite frequencies and τ is the relaxation time of the relaxation mechanism present in the material. Eq. (5) can be written as real and imaginary parts separated as:

$$\varepsilon'(\omega) = \varepsilon_\alpha + \frac{\varepsilon_s - \varepsilon_\alpha}{1 + \omega^2\tau^2} \tag{6}$$

and

$$\varepsilon''(\omega) = (\varepsilon_s - \varepsilon_\alpha)\frac{\omega\tau}{1 + \omega^2\tau^2} \tag{7}$$

Eqs. (6) and (7) are known as Debye equations since they were derived by Debye on a molecular basis [17]. The drop in dielectric permittivity with increase in applied frequency is understood according to Eq. (6). Electronic polarization which is attributed to the dielectric polarization in materials has a relaxation time of the order of 10^{-14} s [18]. Such a small relaxation time does not produce dielectric dispersion at the radio frequency (rf) range where the dielectric measurements were made. It is clear that the kind of relaxation mechanism operating in the frequency regime is different and has a higher relaxation time. Many researchers have attributed the dielectric dispersion in rf regime to interfacial polarization [9,19].

In Fig. 11 the variation of dielectric permittivity (ε') with the nickel content in the composite is plotted for four different frequencies at temperature of 40 °C. Permittivity increases with filler loading almost linearly with all frequencies. The same kind of behaviour is exhibited by the composites at all temperatures. Metallic inclusions in any insulating material enhance the dielectric permittivity of the material as predicted by many theoretical models and verified by experimental results [9,18,19]. Increase in permittivity in nickel–rubber nanocomposites is nearly linear with the percentage of loading of the nickel particles. It is possible to tune the dielectric permittivity to a desired value, and the dielectric loss in the material with nickel loading is small, and this material can be a potential candidate for making capacitors, owing to the possibility of moulding rubber as very thin sheets or films.

The enhancement of dielectric permittivity in metal polymer composites can be understood on the basis of three possible mech-
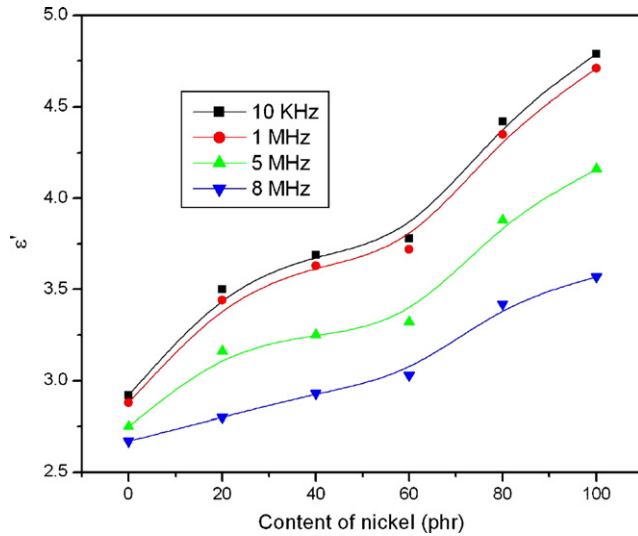

Fig. 9. Variation in strain at breaking stress with filler loading.

Fig. 11. Variation of permittivity with content of nickel in the composites. Per hundred weight ratio of rubber (phr) is plotted in the horizontal axis
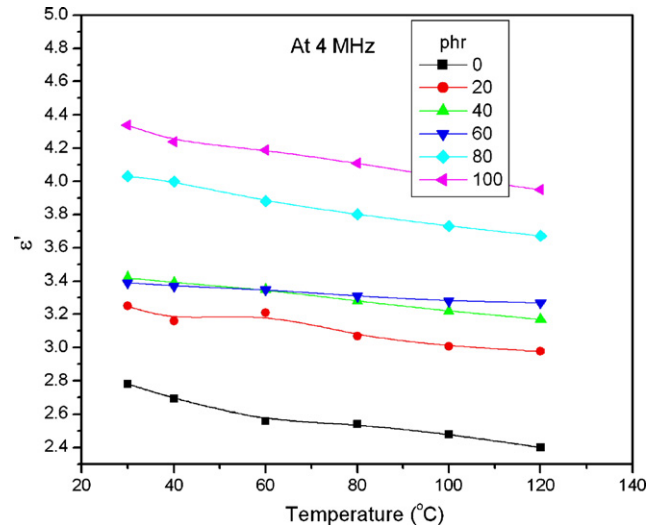

Fig. 12. Variation of dielectric permittivity of the composites with temperature. The plots are that of composites with nickel content of 0–100 phr.

anisms. They are interfacial polarization, enhancement of electrical conductivity and formation of internal barrier layer capacitors (IBLC). Interfacial polarization is always present in materials comprised of more than one phase like a metal elastomer composite. This kind of polarization arising at the interfaces is due to the migration of charge carriers through different phases of the composite material resulting in differential charge accumulation at the interfaces [20]. When these charges are made to move by the application of an external electric field, the motion will be hindered at various points of the composite material differently, causing space charge to appear. The appearance of such space charge can distort the macroscopic field and appears as polarization to an external observer. Interfacial polarization is present in materials with considerable electrical heterogeneity and totally absent in materials which are electrically homogeneous. Hence composite materials will exhibit large interfacial polarization within them under an external electric field. Metal particles embedded in an insulator matrix can act as charge centers and can contribute to the enhancement of dielectric permittivity because of interfacial polarization. Another contributing factor for the enhancement of dielectric permittivity in such composites is the possible increase in the conductivity due to the presence of metal particles in the matrix. But a sharp increase in the conductivity is usually recorded at the percolation threshold of these composites. And below the percolation threshold the increase in conductivity is only moderate or small [10]. However the observed increase in the dielectric permittivity can be a combined effect of these two mechanisms. The enhancement in permittivity can also be due to the formation of IBLC as reported in many systems [21,22]. But in these reports very high value of dielectric permittivity (of the order of 1000) was explained on the basis of IBLC. Even though such an effect was reported in certain polycrystalline ceramics and perovskite materials, IBLC is not a plausible mechanism governing the permittivity in metal elastomer composites.

The variation of dielectric constant with temperature is plotted for various filler loadings at a representative frequency of 4 MHz as depicted in Fig. 12. It was observed that the dielectric permittivity decreased with temperature in the temperature range of 30–120 °C. This effect was found in the blank rubber as well as in the composites. The drop in dielectric permittivity is nearly linear. The change in dielectric permittivity with temperature can be understood in the light of two competing mechanisms. The segmental mobility of the polymer material increases with temperature and this can lead to an increase in the dielectric permittivity. But on the other hand, the thermal expansion of the elastomer material can cause an increase in volume and this can affect the measurement condition as the thickness of the capacitor increases. This can be the cause of the measured decrease in the dielectric permittivity at higher temperatures. The average decrease in the dielectric permittivity over a temperature range of 90 °C is around 7% of the value at room temperature. The linear expansivity of natural rubber is $220 \times 10^{-6}/$°C [23]. The volume expansivity of natural rubber therefore is 660 parts per million (ppm) per °C. Over the temperature range of 90 °C the possible volume expansions are about 6%. This estimation agrees with the observed decrease in the dielectric permittivity with increase of temperature. Differential thermal expansion between the metallic inclusions and the rubber matrix and the resulting disruption of metal clusters had been suggested as a possible reason for the drop in the dielectric permittivity with temperature by some researchers [9]. But a drop in permittivity with increasing temperature found even in blank rubber points to volume expansion as the possible reason. It appears that influence of segmental mobility in the variation of dielectric permittivity is minimal in rubber composites since entire contribution appears to arise from the volume expansion of the rubber matrix.

The dielectric loss of the samples was measured and found increasing with temperature. A plot of dielectric loss against frequency at a temperature of 120 °C is depicted in Fig. 13. The dielectric losses of three samples are shown in this graph; they are blank rubber and rubber loaded with 40 phr and 100 phr of nickel. The loaded samples do not show any dielectric relaxation in the frequency range of the experiments conducted, whereas the blank rubber sample displays a relaxation at about 2.25 MHz.

In Eq. (7) ε_α can be considered equal to the value of dielectric constant obtained at microwave frequencies. Electronic polarization becomes significant at higher frequencies and the value of ε_α remains a constant. The value of ε_s can be determined by extrapolating the dielectric dispersion curve to lower frequencies. Even though we have not attempted to determine the values of ε_α and ε_s it is evident that quantity $\varepsilon_s - \varepsilon_\alpha$ is a constant for a given material and the variation of dielectric loss depends on the relaxation time and the applied frequency only. For rubber samples without any loading we have obtained a peak for the dielectric loss nearly at 2.25 MHz. From Eq. (7) the relaxation time can be calculated.
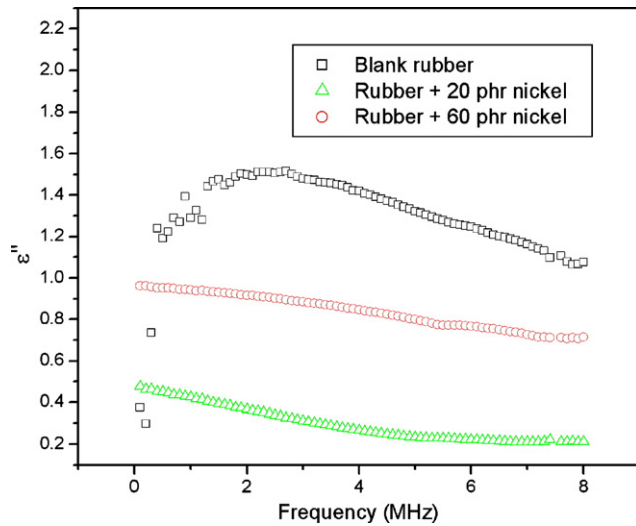
Fig. 13. Variation of dielectric loss with frequency of three samples of composites at a temperature of 120 °C.

The quantity $d\varepsilon''/d\omega$ vanishes when ε'' is maximum and it can be shown that this happens when $\omega\tau = 1$. The relaxation time of blank rubber calculated is nearly 10^{-7} s. Even in blank rubber sample interfacial polarization can be present due to the granular nature of the matrix and due to the presence of unreacted curing agents as impurities. The relaxation process in blank rubber is understood as a weak interfacial polarization. The glass-to-rubber transition of natural rubber occurs at −75 °C and the observed relaxation cannot be due to such a transition [23]. The inclusion of metallic fillers increases the relaxation time of composites, and the peaks go undetected within the frequency range in which the experiments are conducted. It is evident that interfacial polarization suggested by Maxwell–Wagner is responsible for the dielectric dispersion exhibited by these samples in this frequency range. The tendency of other graphs connecting dielectric loss and frequency suggests that a relaxation peak may be observed at some lower frequencies.

In Fig. 14 the dielectric loss is plotted for blank rubber for three temperatures to show its variation with the temperature. It is observed from the graph that the loss increases with the increase in temperature. But the relaxation peak does not shift noticeably
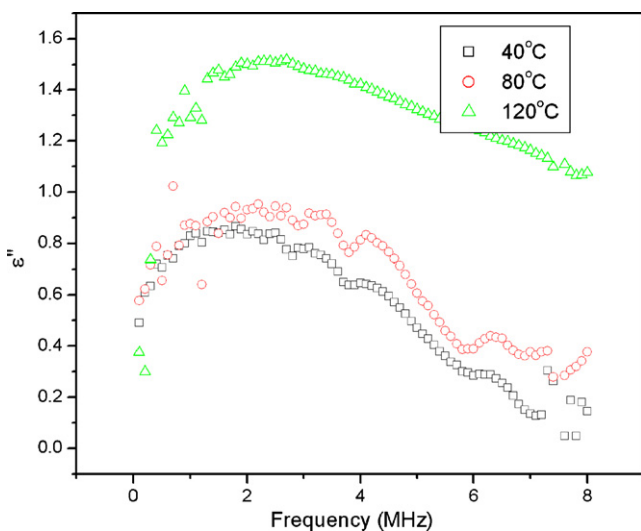
from the 2.25 MHz as indicated by the graphs. It appears that the relaxation time in blank rubber is unaffected noticeably by temperature. The samples loaded with nickel did not show any relaxation as the dielectric loss was found falling with the increase in frequency. It is reasonable to assume that the relaxation time of blank rubber got enhanced when nickel nanoparticles were incorporated in the matrix and relaxation peaks appear at a frequency lower than 100 kHz. Further studies are required to establish the nature of the relaxation phenomenon in nickel-loaded samples at frequencies lower than 100 kHz. Further, at 120 °C the dielectric loss corresponding to the relaxation peak is about 1.5 but it decreased sharply when the temperature is 80 °C to about 0.9. As the frequency increases the loss falls considerably as observed in Fig. 14. So for any frequencies beyond 3 MHz both blank rubber and nickel rubber composite can be considered as low loss materials.

4. Conclusion

Rubber–nickel nanocomposites were synthesized by incorporating nickel nanoparticles in a natural rubber matrix with varying weight percentages of nickel nanoparticles. The magnetic properties of the composite can be tailored by incorporating appropriate amounts of nickel particles. Elastic modulus increased with increase in filler concentration. A dielectric dispersion was observed in the frequency range of 100 kHz to 8 MHz. Dielectric permittivity was found to increase with increase in filler content and decreased with rise in temperature. Interfacial polarization due to the heterogeneity of the samples is attributed as the reason for the variation of dielectric permittivity with frequency as well as filler concentration. High volume expansivity of rubber matrix can be the cause for the variation of permittivity with temperature. Dielectric loss of the composites was found to increase with temperature and a relaxation peak was only observed in blank rubber. For filled samples the dielectric relaxation peaks appear to exist below 100 kHz and further studies are necessary to establish this. A weak interfacial polarization present in the rubber matrix can be attributed to the observance of relaxation peaks in blank rubber.

Acknowledgments

References

[1] T. Tanaka, G.C. Montanari, R. Mulhaupt, IEEE Trans. Dielect. Electr. Insul. II (5) (2004) 763–784.
[2] G.M. Tsangaris, G.C. Psarras, A.J. Kontopoulos, J. Non-Cryst. Solids 131–133 (1991) 1164–1168.
[3] G.C. Psarras, E. Manolakaki, G.M. Tsangaris, Composites Part A 33 (2002) 375–384.
[4] G.C. Psarras, Composites Part A 37 (2006) 1545–1553.
[5] P.S. Neelakanta, Handbook of Electromagnetic Materials, CRC Press, 1995.
[6] B. Zhang, Y. Feng, J. Xiong, Y. Yang, H. Lu, IEEE Trans. Magn. 42 (7) (2006) 1778–1781.
[7] S. Sindhu, M.R. Anantharaman, B.P. Thampi, K.A. Malini, P. Kurian, Bull. Mater. Sci. 25 (7) (2002) 599–607.
[8] M.R. Anantharaman, S. Sindhu, S. Jagatheesan, K.A. Malini, P. Kurian, J. Phys. D: Appl. Phys. 32 (15) (1999) 1801–1810.
[9] Z.M. Elimat, A.M. Zihlif, G. Ragosta, J. Phys. D: Appl. Phys. 41 (2008) 165408.
[10] Z.M. Dang, C.W. Nan, D. Xie, Y.H. Zhang, S.C. Tjong, Appl. Phys. Lett. 85 (2004) 97–99.
[11] R.K. Sahu, A.K. Ray, S.K. Das, A.J. Kailath, L.C. Pathak, J. Mater. Res. 21 (7) (2006) 1664–1673.
[12] K.A. Malini, P. Kurian, M.R. Anantharaman, Mater. Lett. 57 (2003) 3381–3386.
[13] E.M. Mohammed, M.R. Anantharaman, J. Instrum. Soc. India 32 (3) (2002) 165.
[14] H.V. Keer, Principles of Solid State Physics, Wiley Eastern Ltd., New Delhi, 1998.
[15] W. Gong, H. Li, Z. Zhao, J. Chen, J. Appl. Phys. 69 (1991) 5119.

Fig. 14. Graph showing the dielectric loss at temperatures 40 °C, 80 °C and 120 °C of blank rubber.

[16] N.H.H. Abu Bakar, J. Ismail, M. Abu Bakar, Mater. Chem. Phys. 104 (2007) 276–283.
[17] I.I. Perepechko, An Introduction to Polymer Physics, Mir Publishers, Moscow, 1981.
[18] B. Tareev, Physics of Dielectric Materials, MIR Publishers, Moscow, 1975.
[19] S.M. Musameh, M.K. Abdelazeez, M.S. Ahmad, A.M. Zihlif, M. Malinconico, E. Martuscelli, G. Ragosta, Mater. Sci. Eng.: B 10 (1) (1991) 29–33.
[20] H.A. Pohl, Dielectrophoresis, Cambridge University Press, London, 1978.
[21] D.C. Sinclair, T.B. Adams, F.D. Morrison, A.R. West, Appl. Phys. Lett. 80 (2002) 2153.
[22] P.K. Jana, S. Sarkar, H. Sakata, T. Watanabe, B.K. Chaudhuri, J. Phys. D: Appl. Phys. 41 (2008) 65403.
[23] C.M. Blow, C. Hepburn, Rubber Technology and Manufacture, second ed., Butterworths, London, 1982, p. 347.